

# Imaging obscured subsurface inhomogeneity using laser speckle

Ralph Nothdurft, Gang Yao

*Department of Biological Engineering, University of Missouri-Columbia, Columbia, MO 65211*  
[renothdurft@mizzou.edu](mailto:renothdurft@mizzou.edu), [yaog@missouri.edu](mailto:yaog@missouri.edu)

**Abstract:** We have developed a laser speckle imaging method to reveal obscured subsurface inhomogeneities that cannot be seen under incoherent illumination. Speckle images of a scattering object were generated under coherent illumination using a laser. A sequence of speckle images was acquired with fixed exposure time and acquisition interval. The temporal statistics of each pixel in the image sequence was calculated and formed a new image. We demonstrate that such temporal speckle contrast images can reveal obscured subsurface objects. More importantly, by controlling image acquisition parameters, surface inhomogeneity can be eliminated in order to better bring to view the subsurface objects.

©2005 Optical Society of America

**OCIS codes:** (030) Coherence and statistical optics; (110.6150) Speckle imaging; (290.4020) Multiple scattering; (290.7050) Turbid media.

---

## References and links

1. L. Wang, P. P. Ho, G. Liu, G. Zhang, and R. R. Alfano, "Ballistic 2-D imaging through scattering wall using an ultrafast Kerr gate," *Science* **253**, 769-771 (1991).
2. M. D. Duncan, M. Bashkansky, and J. F. Reintjes, "Subsurface defect detection in materials using optical coherence tomography," *Opt. Express* **2**, 540-545 (1998), <http://www.opticsexpress.org/abstract.cfm?URI=OPEX-2-13-540>
3. M. A. O'Leary, D. A. Boas, B. Chance, and A. G. Yodh, "Experimental images of heterogeneous turbid media by frequency-domain diffusing-photon tomography," *Opt. Lett.* **20**, 426-428 (1995).
4. R. Nothdurft, G. Yao, "Expression of target optical properties in subsurface polarization-gated imaging," *Opt. Express* **13**, 4185-4195 (2005), <http://www.opticsexpress.org/abstract.cfm?URI=OPEX-13-11-4185>.
5. J. Li, G. Yao, L.H.V Wang, "Degree of polarization in laser speckles from turbid media: Implications in tissue optics," *J. Biomed. Opt.* **7**, 307-312 (2002).
6. J. Rosen, D. Abookasis, "Seeing through biological tissues using the fly eye principle," *Opt. Express* **11**, 3605-3611 (2003), <http://www.opticsexpress.org/abstract.cfm?URI=OPEX-11-26-3605>.
7. S. Yuan, A. Devor, D.A. Boas, A.K. Dunn, "Determination of optimal exposure time for imaging of blood flow changes with laser speckle contrast imaging," *Appl. Opt.* **44**, 1823-1830 (2005).
8. T.F. Begemann, G. Glker, K.D. Hinsch, K. Wolff, "Corrosion monitoring with speckle correlation," *Appl. Opt.* **38**, 5948-5955 (1999).
9. M. Pajuelo, G. Baldwin, H. Rabal, N. Cap, R. Arizaga, M. Trivi, "Bio-speckle assessment of bruising in fruits," *Opt. Lasers Eng.* **40**, 13-24 (2003).
10. G. H. Sendra, R. Arizaga, H. Rabal, and M. Trivi, "Decomposition of biospeckle images in temporary spectral bands," *Opt. Lett.* **30**, 1641-1643 (2005).
11. H. Cheng, Q. Luo, S. Zeng, S. Chen, J. Cen, and H. Gong, "Modified laser speckle imaging method with improved spatial resolution," *J. Biomed. Opt.* **8**, 559-564 (2003).

---

## 1. Introduction

Imaging obscured subsurface objects is a critical task in many fields such as material defect detection and security inspection. Optical imaging has attracted much attention because of its many advantages such as non-contact, non-invasive, and high speed. Unfortunately, many materials are highly scattering which randomizes the light trajectories and thus obscures embedded objects. To address such multiple scattering problems, a variety of optical techniques has been developed. These techniques include time-resolved measurements using ultra-short pulse lasers [1], optical low coherence tomography [2], frequency-domain tomography [3], and polarization imaging [4]. Although excellent progress has been made by

using these techniques, they typically require either expensive systems or specialized components. In this study we used common laboratory components to examine data often discarded as noise, i.e. the optical speckle patterns, for imaging obscured subsurface inhomogeneities.

Optical speckle can be generated when coherent light is scattered from a rough surface or turbid volume [5]. Due to its grainy appearance, speckle is traditionally considered as a noise source to image formation and multiple-averaging is usually applied to smooth out the coarse speckle patterns [6]. On the other hand, many studies have indicated that the speckle patterns contain important information of the underlying medium. Speckle patterns often change with time because of the movement of speckle generating objects. The resulting dynamic speckle can be used to derive information related to the movement and to characterize certain material properties. Dynamic speckle has been used in applications such as flow detection [7], corrosion detection [8], and biological activity diagnosis [9]. Recently, Sendra *et al.* [10] found that different biological activities can be revealed by filtering dynamic speckle images.

In this study, we demonstrated that laser speckle can be applied to image obscured subsurface inhomogeneities that are invisible when illuminated using incoherent light. More importantly, by controlling image acquisition conditions, surface inhomogeneities can be eliminated from the image in order to better bring to view the subsurface obscured objects.

## 2. Materials and methods

Figure 1 shows a diagram of the experimental setup. A He-Ne laser (NT55-467, Edmund Optics Inc., Barrington, NJ) provided polarized, coherent light at 633nm wavelength. The laser outputs a maximal power of 20mW as measured with a power meter (2835-C, Newport Corporation, Irvine, CA) equipped with an integrating sphere detector (818-IS, Newport Corporation, Irvine, CA). Rotating a linear polarizer in the laser path provided control over beam intensity. The laser beam size was expanded to illuminate a 20mm sample area at 45° incidence. In order to compare laser speckle image with incoherent imaging, a 150W compact fluorescent bulb was used to provide a uniform diffuse light. Targets were placed on the flat surface of an optical table. Light returning from the target was captured at normal incidence by a black and white video CCD camera (TM-7AS, Pulnix, Sunnyvale, CA) with a 640x480 pixel array. A 1:2.8, 50mm video lens was used so that the camera aperture accepted photons within 1.7° over a 16mm by 12mm imaging area. A fixed aperture of f/11 was used throughout the experiments. Within the lens assembly a 633nm filter was used to reject ambient light and assure comparison of equivalent wavelengths when the broadband incoherent light source was used. A sequence of images was acquired with fixed exposure time and interval. The images were digitized by an 8-bit frame grabber (PCI-1704, National Instruments, Austin, TX) and processed by a computer.

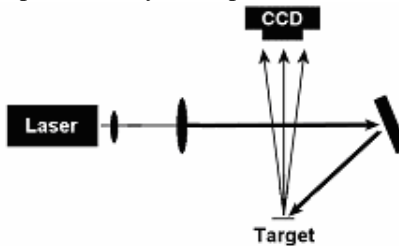


Fig. 1. Schematic diagram of experimental setup.

The temporal speckle contrast image was constructed by calculating the ratio of standard deviation and mean value of each image pixel in the time sequence. The value of pixel ( $i, j$ ) in the speckle contrast image was calculated as:

$$C_{i,j} = \frac{\sqrt{\frac{1}{N-1} \sum_{t=0}^T (X_{i,j}^t - \bar{X}_{i,j})^2}}{\bar{X}_{i,j}} \quad (1)$$

where the numerator is the standard deviation of the sequence and the denominator is the mean value of the sequence.  $X_{i,j}^t$  is the  $(i, j)$  pixel of the image acquired at time  $t$ ;  $N$  is the total number of images acquired in the sequence;  $t_0$  is the time that the first image in the sequence was acquired; and  $T$  is the time that the last image in the sequence was acquired. The time interval  $\Delta t$  between two consecutive images was fixed in the experiments.  $\bar{X}_{i,j}$  is the mean value of pixel  $(i, j)$  in the time averaged speckle image:

$$\bar{X}_{i,j} = \frac{1}{N} \sum_{t=t_0}^T X_{i,j}^t \quad (2)$$

The temporal speckle statistics in the form of Eq. (1) is analogous to the classical concept of speckle contrast, which is defined in spatial domain and applied to calculate the spatial characteristics of a speckle pattern [5]. A similar method [11] was used previously in laser speckle imaging of blood flows where the blood vessels were not obscured and can be seen also under incoherent illumination.

### 3. Results

Several objects were used to demonstrate this technique. Figure 2 shows the imaging result of a 5mm void hole of an optical table covered by a piece of white paper (thickness 0.12mm). The paper was laid on the table by its own weight without any clamping. Fifty 4-millisecond captures with 200ms separation were collected. The top and bottom rows are for incoherent and coherent light respectively. In the mean images no object is visible with either light source. In the display each image is mapped with an optimal local palette by scaling the pixel values to cover the full 8-bit dynamic range. This mapping accentuates surface details in the incoherent image and the inhomogeneous intensity distribution in the laser speckle image. The grainy appearance induced by speckle is significantly reduced by the multiple averaging. In the standard deviation images the void hole becomes visible under coherent illumination, while the incoherent image shows only a uniform background. Finally the speckle contrast image enhances the target appearance and smoothes out the inhomogeneous background.

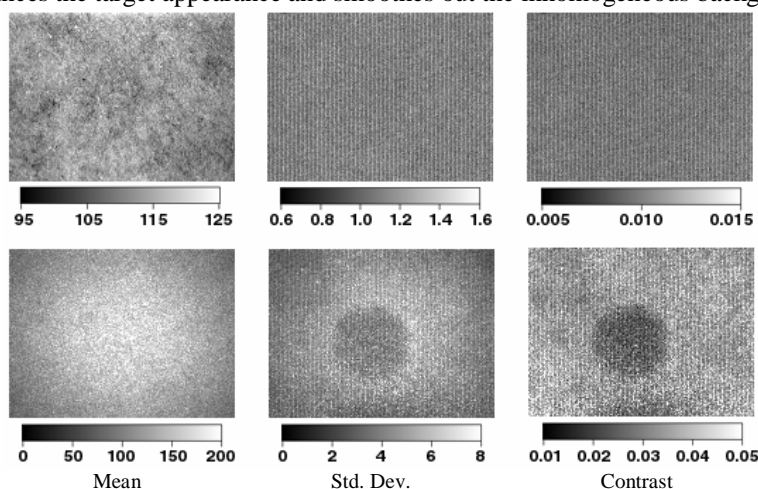


Fig. 2. Images of an obscured void hole underneath a white paper. Images listed in the 1<sup>st</sup> row were acquired with incoherent white light illumination; whereas imaged in the 2<sup>nd</sup> row were acquired using laser illumination.

Figure 3 shows the application of the technique to other targets. Figure 3(a) and 3(b) are the incoherent image and temporal speckle contrast image of white and black paint squares on the underside of a 0.12mm sheet paper. Under incoherent light illumination, the black paint can be seen; whereas the white paint is barely visible. Again, these paint objects are clearly visible with better contrast and resolution in the temporal speckle contrast image. The black

paint appears darker in Fig. 3(b). Some surface inhomogeneities on the white paint can be identified.

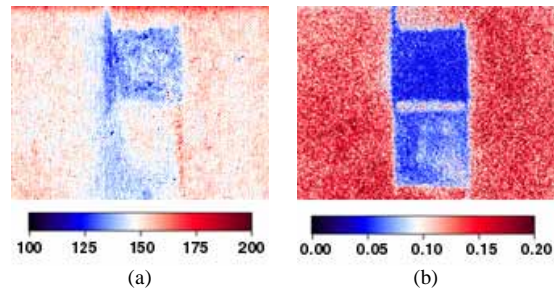


Fig. 3. Images of obscured black paint and white paint objects. (a) Incoherent image; (b) Temporal speckle contrast image.

In practice, there are usually substantial surface inhomogeneities that block the view of subsurface targets. In order to test whether these surface objects can be eliminated using appropriate image capture parameters, we conducted studies using a simple model consisting of a 0.24mm thick paper with off-diagonal squares printed on both the front surface and back surface (Fig. 4). The images in Fig. 4(a) and 4(b) were acquired using the maximal output laser power. The camera exposure time and frame interval are 1/250s and 50ms, respectively. In the averaged speckle image or incoherent image, the squares printed on front surface are visible (Fig. 4(a)); their counterparts on the reverse side become visible in the speckle contrast image (Fig. 4(b)). This offset square target represents a simple model of the many targets we expect to encounter that have both surface and subsurface inhomogeneities. Therefore we examined its behavior in detail.

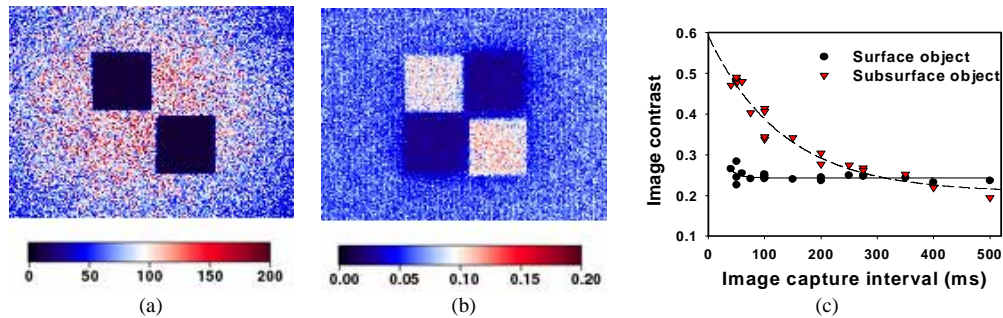


Fig. 4. Targets for examining the effect of image capture parameters. (a) Averaged speckle images; (b) Temporal speckle contrast image; (c) Image contrast changes with acquisition interval.

We found the speckle contrast changes significantly when varying the image capture parameters. The primary factors that influence the imaging of hidden targets in Fig. 4 are shutter speed (or exposure time), incident power, and time interval between subsequent capture. A longer exposure time is equivalent to more temporal averaging, thus smooths out the speckle pattern and reduces the standard deviation. A higher illumination light intensity also reduces the speckle contrast probably due to increasing thermal activities. Increasing either the shutter time or incident power seems to increase the visibility of the hidden target. For a given product ( $P$ ) of shutter speed ( $S$ ) and incident power ( $I$ ),  $P = S \times I$ , the speckle contrast behavior is effectively constant. Most significantly, the surface target and subsurface target show a different dependence on these factors, which indicates that the acquired speckle patterns depend on both the surface and subsurface conditions of the target. This phenomenon is important because the image appearance is essentially determined by the relative speckle contrast among the background, the surface and the subsurface inhomogeneities. As an

example, Fig. 4(c) shows the calculated object contrast of the temporal speckle contrast image (Fig. 4(b)) at different time intervals between two consecutive captures, while keeping the exposure time and illumination power at the same values as in Fig. 4(b). The target contrast was calculated as the relative pixel value difference between the object and the surrounding background:  $|O-B|/|O+B|$ , where  $O$  is the object pixel value and  $B$  is the background pixel value. It can be seen that at shorter capture intervals, the obscured target has larger contrast difference than the surface target. At longer capture intervals, they have similar imaging contrast values.

By tuning the capture parameters, the image contrast values of the surface and subsurface targets can be changed. When the contrast of the surface inhomogeneity is within the noise level of the background image, the surface effect is essentially removed from the image. Figure 5 shows an example where a page from a lab manual (0.14mm thickness) was used as the target. The camera settings are similar to those used in Fig.4 with full laser power. There are black printed words on both sides of the paper. Fig. 5(a) shows the mean speckle images where the printed words on the surface and a straight line at the bottom are visible. In the standard deviation image (Fig. 5(b)), there are some obscured characters at the back of the paper where the first line is "This is in lieu". However, the words on the front surface significantly block the second line of words. In the speckle contrast image (Fig. 5(c)), the characters on the front surface are removed, while the characters at the back surface are revealed. The second line is "(o)r implied, an(d)", and the third line is "(co)nsequential".

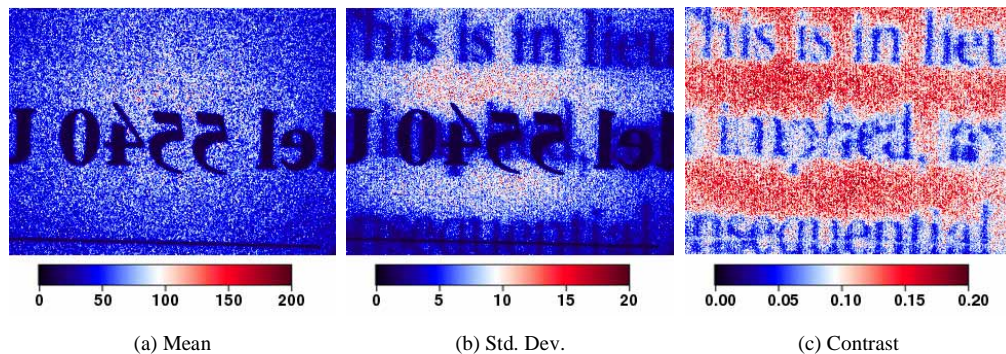


Fig. 5. Images of a piece of paper with printed words on both sides. (a) Multiply-averaged laser image; (b) The standard-deviation image; (c) The temporal speckle contrast image. The images were horizontally flipped to display the obscured words on the back surface in readable order.

#### 4. Conclusion

It is understood that dynamic speckle patterns are generated by small movements of the target. In our case, the speckle dynamic behavior was most likely due to the heat generated Brownian motion induced by absorption of the light energy. Therefore the inhomogeneous absorption properties of the target affect the speckle dynamics. For example, the dark object has a low speckle contrast owing to increased thermal activity from absorption. Both the surface and subsurface inhomogeneities change the observed speckle patterns. On the other hand, at certain image acquisition conditions, speckle patterns with different temporal statistics appear differently. Therefore, it is possible to differentiate objects by controlling image acquisition parameters. Because environmental conditions were not controlled in our study, temperature fluctuations and small air flow may have also contributed to speckle dynamics. In addition, system noise performance also affects speckle contrast. For example, a higher camera gain can increase the noise level which has an impact on standard deviation of dark objects. To what extent the image contrast of different objects can be manipulated in the speckle-contrast image need further investigation. We have shown, however, that a number of significantly

varied targets can be detected by controlling common capture parameters such as the exposure time and time interval between subsequent acquisitions.

In conclusion, we found that the temporal characteristics of dynamic speckle can be utilized to reveal obscured subsurface objects. It was noted that the image resolution obtained with this method was still limited by the optical speckle phenomenon. This method, however, is simple to implement and could be potentially applied as a rapid imaging screening tool in material defect monitoring and security inspections.

### **Acknowledgments**

This research was made possible by a research board grant from the University of Missouri-Columbia.